Title: Time-delayed effects of a single application of AgNPs on structure of testes and functions in Blaps polychresta Forskal, 1775 (Coleoptera: Tenebrionidae)

Author: Hussein K. Hussein, Karolin K. Abdul-Aziz, Eman H. Radwan, Nahed R. Bakr, Abeer El Wakil, Maria Augustyniak [i in.]

UNIWERSYTET ŚLĄSKI W KATOWICACH

Biblioteka Uniwersytetu Śląskiego

Ministerstwo Nauki i Szkolnictwa Wyższego

Time-delayed effects of a single application of AgNPs on structure of testes and functions in *Blaps polychresta* Forskal, 1775 (Coleoptera: Tenebrionidae)

Lamia M. El-Samad [a,1], Saeed El-Ashram [b,c,d,1], Hussein K. Hussein [a], Karolin K. Abdul-Aziz [e], Eman H. Radwan [e], Nahed R. Bakr [e], Abeer El Wakil [f], Maria Augustyniak [g,*]

[a] Department of Zoology, Faculty of Science, Alexandria University, Alexandria, Egypt
[b] College of Life Science and Engineering, Foshan University, 18 Jiangwan Street, Foshan 528231, Guangdong Province, China
[c] Faculty of Science, Kafrelsheikh University, Kafr El-Sheikh 33516, Egypt
[d] Department of Poultry Science, University of Arkansas, Fayetteville, AR, USA
[e] Department of Zoology, Faculty of Science, Damanhour University, Egypt
[f] Biological and Geological Sciences Department, Faculty of Education, Alexandria University, Egypt
[g] Institute of Biology, Biotechnology and Environmental Protection, Faculty of Natural Sciences, University of Silesia in Katowice, Bankowa 9, 40-007 Katowice, Poland

HIGHLIGHTS

- The LD50 for silver nanoparticles (AgNPs) for *Blaps polychresta* is 0.05 mg/g b.w.t.
- A single application of AgNPs caused increased apoptosis but not necrosis in the testes.
- AgNPs caused a time-delayed decrease in antioxidant enzyme activity in *B. polychresta*.
- Severe degeneration of the testes 30 days after the AgNP single injection was described.
- AgNPs can become a long-lasting stable Ag^+ ion source in *B. polychresta* cells.

GRAPHICAL ABSTRACT
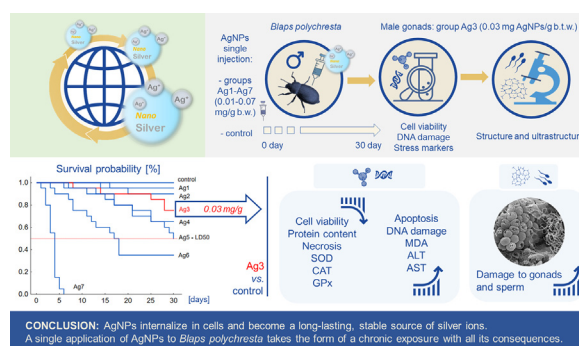
ARTICLE INFO

ABSTRACT

Silver nanoparticles (AgNPs) are currently the most frequently used engineered nanoparticles. The penetration of AgNPs into ecosystems is undeniable, and their adverse effects on organism reproduction are of fundamental importance for ecosystem stability. In this study, the survival time of the Egyptian beetle *Blaps polychresta* Forskal, 1775 (Coleoptera: Tenebrionidae), after a single application of 7 different doses, was calculated for 30 days. Then, for the group for which the effect on mortality was calculated as LOAEL - the Lowest Observed Adverse Effect Level, namely, 0.03 mg AgNPs/g body weight (b.w.t.), the following were assessed: structure and ultrastructure of gonads by TEM and SEM, cell viability by cytometry, DNA damage by the comet assay, and a variety of stress markers by spectrophotometric methods. A dose-dependent reduction in the survival time of the insects was

Abbreviations: NPs, nanoparticles; AgNPs, silver nanoparticles; NiO-NPs, nickel oxide nanoparticles; TiO₂NPs, titanium dioxide nanoparticles; ZnONPs, zinc oxide nanoparticles; AuNPs, gold nanoparticles; TEM, transmission electron microscopy; EDX, Energy-dispersive X-ray; SEM, scanning electron microscopy; ROS, reactive oxygen species; PC, protein content; AST, aspartate aminotransferase; ALT, alanine aminotransferase; MDA, malondialdehyde; SOD, superoxide dismutase; CAT, catalase; GPx, glutathione peroxidase; GST, glutathione S-transferase; NOEL, no observed effect level; LOEL, lowest observed effect level; LOAEL, the Lowest Observed Adverse Effect Level; EDTA, ethylenediaminetetraacetic acid; DMSO, dimethyl sulfoxide; TBA, 2-thiobarbituric acid; TBARS, 2-thiobarbituric acid-reactive substance; cumOOH, cumene hydroperoxide; GSH, reduced glutathione; CDNB, 1-chloro-2,4-dinitrobenzene.

* Corresponding author.
E-mail address: maria.augustyniak@us.edu.pl (M. Augustyniak).
[1] These authors contributed equally in the study.

revealed. Detailed analysis of the testes of beetles treated with 0.03 mg AgNPs/g b.w.t. revealed numerous adverse effects of nanoparticles in structure and ultrastructure, accompanied by increased apoptosis (but not necrosis), increased DNA damage, increased lipid peroxidation, and decreased levels of antioxidant enzymes. Most likely, the observed results are connected with the gradual release of Ag^+ from the surface of the nanoparticles, which, once applied, are internalized in cells and become a long-lasting, stable source of Ag^+ ions. Thus, a single exposure to AgNPs may have the effects of chronic exposure and lead to structural damage and dysfunction of the gonads of *B. polychresta*.

1. Introduction

Silver nanoparticles (AgNPs), due to their exceptional, catalytic, electronic, and optical properties but, most of all, antibacterial properties, are currently the most frequently used nanoparticles (NPs). Approximately 435 currently produced nanoproducts contain silver, which is approximately one-fifth of all currently produced types of nanomaterials (Tortella et al., 2020). AgNPs are widely used in medicine, stomatology, cosmetology, fabric and clothing production, washing machines, various commercial products, medical devices, food packaging, and many other applications, as well as for environmental purposes, such as wastewater treatment or bioremediation (Rai et al., 2009; Wei et al., 2015; Pulit-Prociak and Banach, 2016; McGillicuddy et al., 2017; Tortella et al., 2020).

Undoubtedly, AgNPs influence the development of technology and bring many benefits. However, this issue has another face. The same properties of AgNPs, which are used to improve the quality of life, can become a serious risk to ecosystems and organisms living in them, including humans. The fabrication and use of AgNP-containing products are associated with the production of sewage and waste, which finally reach aquatic and terrestrial environments, where they may undergo various modifications that intensify or weaken their biological activity. The final toxic effect of AgNPs depends on many factors and environmental conditions (McGillicuddy et al., 2017; Guo et al., 2018; Shevlin et al., 2018; Bhargava et al., 2021). Various chemical transformations can alleviate AgNP toxicity by reducing their availability and decreasing silver ion release. However, AgNPs are known to be able to accumulate in various organisms and then be transferred along the food web to higher trophic levels (Tortella et al., 2020; Dang et al., 2021; Khodaparast et al., 2021). The gradual and slow release of silver ions from AgNPs gives reason to assume that even a single exposure may cause long-term effects. Thus, the delayed time-cumulative toxicity of AgNPs is the main thread of this study.

Currently, the toxicity of AgNPs is believed to be related mainly to the oxidation of the particle surface and the release of silver ions. However, scientists are still deliberating how the nano form and the ionic form contribute to the overall toxicity (McShan et al., 2014). The effects of coexisting particles and the surface coating type on the toxicity of AgNPs are also not entirely clear. The commonly accepted mechanism of AgNP toxicity is based on the intensification of free radical generation and the increase in oxidative stress (McShan et al., 2014). The consequences are typical, i.e., damage to biomolecules, including proteins, lipids, and nucleic acids, redox imbalance, alteration of antioxidant enzyme activity, and damage to membranes and organelles (McShan et al., 2014). These disorders are reflected in the general condition of an organism, often manifested by disturbances in the amount of food consumed and energy absorption (Seyed Alian et al., 2021). Further consequences include disturbance of growth and other organism functions, including reproduction.

Adverse effects of AgNPs on reproductive functions are of fundamental importance for a species. They can lead to population number decline and ecosystem imbalance, including the extinction of a particular, sensitive species. Effects of NPs on gonads were found in male and female rodents. Studies conducted mainly on rats or mice show that NPs can penetrate the testes, prostate gland, and epididymis with the circulating blood, causing damage to their structure and disrupting

organ function (Wang et al., 2018). However, there are also articles showing that injection of 70 nm gold core-silica shell NPs into mice did not lead to the internalization of these nanoparticles in the testes (Leclerc et al., 2015). AgNPs can affect Leydig cell function and cause increased testosterone levels, decreased sperm counts, and multiple morphological dose- and size-dependent changes in rodents (Gromadzka-Ostrowska et al., 2012; Garcia et al., 2014). Importantly, oral exposure appears to be less dangerous, at least in sperm parameters such as motility, viability, and morphology (Lafuente et al., 2016).

Data on the influences of NPs on the structure and functions of insect gonads are scarce. Most of the tested NPs tend to induce various gonadal lesions and disturb reproductive functions, especially when administered at higher doses/concentrations. Histological changes in gonads caused by NPs are often accompanied by increased apoptosis, a reduced number of viable cells, and many other consequences typical of oxidative stress (Ni et al., 2015; Dziewięcka et al., 2017; Raj et al., 2017; Dziewięcka et al., 2018; Karpeta-Kaczmarek et al., 2018; Dziewięcka et al., 2020; El-Ashram et al., 2020; Flasz et al., 2020; Flasz et al., 2021; Kheirallah et al., 2021). However, it is possible, especially when using low doses of NPs, to enhance the reproduction and fecundity of insects (Ni et al., 2015).

In light of the aforementioned information, this study aimed to determine the dose-survival relationship in a wild insect, *Blaps polychresta*, after a single application of AgNPs and evaluate its delayed effects, measured 30 days after exposure to a sublethal dose, on selected molecular, cellular, and tissue parameters in male gonads of this species.

2. Materials and methods

2.1. Hypothesis

We decided to test the following hypotheses:

H0: A single application of AgNPs at a sublethal dose does not cause adverse changes in the structure and function of male *B. polychresta* gonads and does not significantly affect the level of stress markers in this organ. The acceptance of this hypothesis can be explained by the tendency of AgNPs to agglomerate and coat with various substances. A single administration of AgNPs may initially stimulate an antioxidant response and induce beneficial changes in the organism. However, once the particles are immobilized and coated, they become safe.

H1: AgNPs administered at a single low dose disturb the homeostasis of the organism, which is manifested by changes in the level of stress markers and/or the intensification of damage to molecules (including proteins, lipids, and DNA) and/or increased incidence of cell death (including apoptosis) and/or changes in the structure and ultrastructure of the gonads. The premise for accepting this hypothesis is the gradual release of Ag^+ from the surface of nanoparticles, which, once applied, internalize in cells and become a long-lasting stable source of silver ions. From this perspective, one-time exposure can be viewed as chronic exposure with all its consequences.

2.2. Insects

Tenebrionid beetles (Coleoptera) are a good research model due to their cosmopolitan nature, significant importance in ecosystems, large

size, and relatively high resistance to experimental treatments (Kheirallah et al., 2019; Kheirallah and El-Samad, 2019). *Blaps polychresta* has been described as a successful indicator of industrial pollution (Osman et al., 2015; Osman and Shonouda, 2017; Kheirallah and El-Samad, 2019).

The beetles (Fig. 1a) used in the experiment were collected at the garden of the Faculty of Science (Elshatby, Alexandria University, Alexandria, Egypt) and identified as *B. polychresta* Forskal, 1775 (Coleoptera: Tenebrionidae). The area of insect collection is considered unpolluted (Kheirallah et al., 2021). After approximately 320 adult specimens were collected in the field, insects were transferred to the laboratory, where sex identification was performed based on the differences in length and shape of the mucro, a caudal extension at the apex of the elytra (Soldati et al., 2017). Finally, 160 males were selected for the study and placed in cages filled with soil from the insect collection site. The insects were kept in controlled conditions (temperature 29 ± 3 °C and 85% RH) similar to the natural environment. The mean body weight of an adult male beetle was 2.07 g. After an acclimation period of 5 days, males were randomized into experimental groups of 20 in each group. A control group and seven groups treated with AgNPs at various concentrations were created. The females were returned to their natural habitat.

2.3. Preparation of AgNPs suspension

AgNPs were purchased from Sigma–Aldrich Co. Ltd. (St. Louis, MO, USA). The characterization of AgNPs was performed using transmission electron microscopy (TEM) (JEOL, JEM-2100; JEOL USA, Inc.) at an accelerating voltage of 200 kV. The electron micrographs (Fig. 2a) revealed the presence of single spherical structures and aggregates. The diameter of a single nanoparticle ranged from 5.23 to 24.85 nm (mean 20.04 ± 2.36 nm), which was in line with the manufacturer's declaration (<50 nm).

A stock suspension of AgNPs (1 mg/mL) was prepared in normal saline. The suspension was sonicated using a Branson 450 sonicator (Branson Ultrasonics Crop, Danbury, CT, USA). Sonication was carried out on ice (100% amplitude, 20 kHz frequency) for 10 min in the following cycles: 8 s - operate and 2 s - standby. The stock suspension was used to prepare working solutions from which doses were prepared, and the final volume of the dose was adjusted to the mass of individuals.

2.4. Experimental design

In the first stage of the study, we aimed to determine the LD50 of AgNPs for *B. polychresta*. Adult males were injected with a suspension of AgNPs at various doses. Seven groups (named Ag1-Ag7) were created receiving AgNPs at final doses of 0.01, 0.02, 0.03, 0.04, 0.05, 0.06, and 0.07 mg/g body weight. The control group was injected with normal saline. The injection procedure was performed according to the method described by Leonard et al. (1985) adapted to the species under investigation (Kheirallah et al., 2021). Briefly, after gentle anesthesia of the insects on ice (the individuals were placed in Petri dishes on ice for ~10 min), a puncture (1 mL BD hypodermic syringe; 27G, 1″2/needle) was performed at the ventro-caudal area through the arthrodial membrane between the 4th and 5th abdominal sclerites. During puncture and gentle injection of the suspension, the needle was kept horizontal to minimize possible internal damage (de Viedma and Nelson, 1977; Kheirallah et al., 2021). After this treatment, the insects were placed back in cages with soil and kept under controlled conditions. Insect mortality was monitored daily for 30 days. Based on the obtained results, survival time was calculated by Kaplan–Meier analysis, and the LD50 was estimated (Plata-Rueda et al., 2020).

Further biochemical and histological analyses were performed on Ag3 group individuals. The survival in the Ag3 group 30 days after the injection was 75%. This dose was assumed to be the Lowest Observed Adverse Effect Level (LOAEL) for mortality, taking mortality as the endpoint. Thus, the mortality effect of 25% gave premises for an in-depth examination of stress markers and the evaluation of potential histological and ultrastructural changes in beetles from the Ag3 group.

2.5. Ag X-ray detection in the testes of B. polychresta

To determine the percentage of Ag content in *B. polychresta* testes (Fig. 2b), energy dispersive X-ray (EDX) microanalysis at the Electron Microscope Unit (EM), Faculty of Science, Alexandria University, Egypt, was used. The EDX analyses integrated the characteristics of the scanning electron microscope (SEM; JEOL JSM-5300). Randomly selected individuals from the control or Ag3 groups were anesthetized on ice, the testes were gently dissected, and slides (Fig. 2c) were
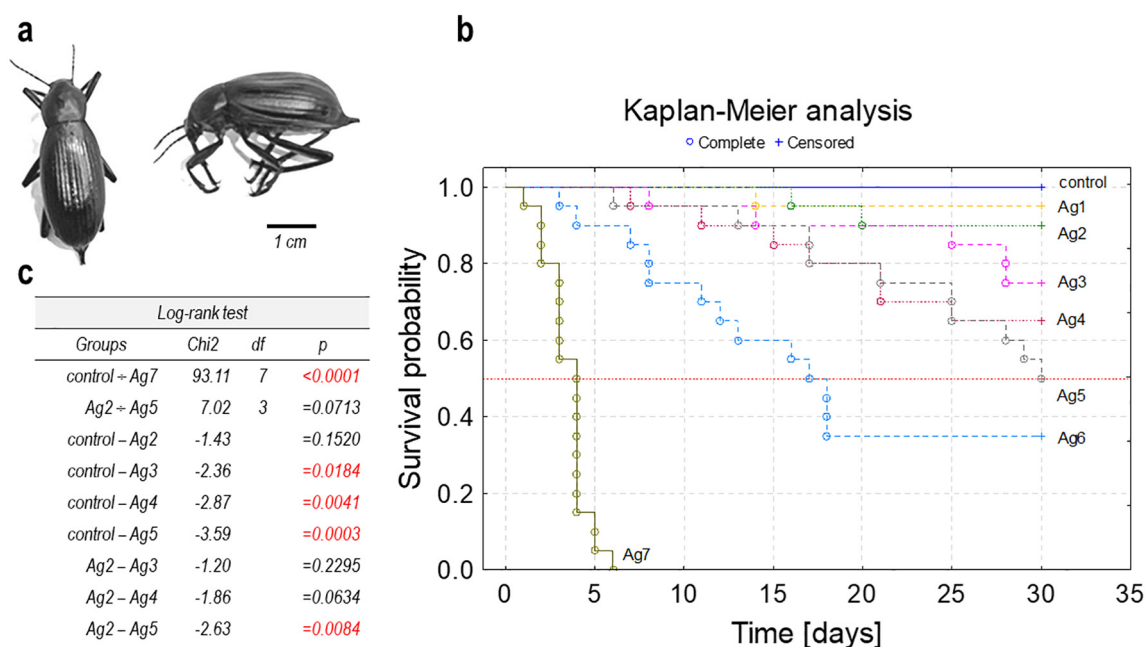

Log-rank test			
Groups	Chi2	df	p
control ÷ Ag7	93.11	7	*<0.0001*
Ag2 ÷ Ag5	7.02	3	*=0.0713*
control – Ag2	-1.43		*=0.1520*
control – Ag3	-2.36		*=0.0184*
control – Ag4	-2.87		*=0.0041*
control – Ag5	-3.59		*=0.0003*
Ag2 – Ag3	-1.20		*=0.2295*
Ag2 – Ag4	-1.86		*=0.0634*
Ag2 – Ag5	-2.63		*=0.0084*

Fig. 1. Survival probabilities of *Blaps polychresta* (a) during 30 days after exposure to silver nanoparticles at the following doses 0.01, 0.02, 0.03, 0.04, 0.05, 0.06, and 0.07 mg·g^{-1} body weight (Ag1, Ag2, Ag3, Ag, 4, Ag5, Ag6, and Ag7 groups, respectively). Kaplan-Meier survival analysis for all experimental groups (b) and results of Log-rank test (c). (For interpretation of the references to colour in this figure legend, the reader is referred to the web version of this article.)
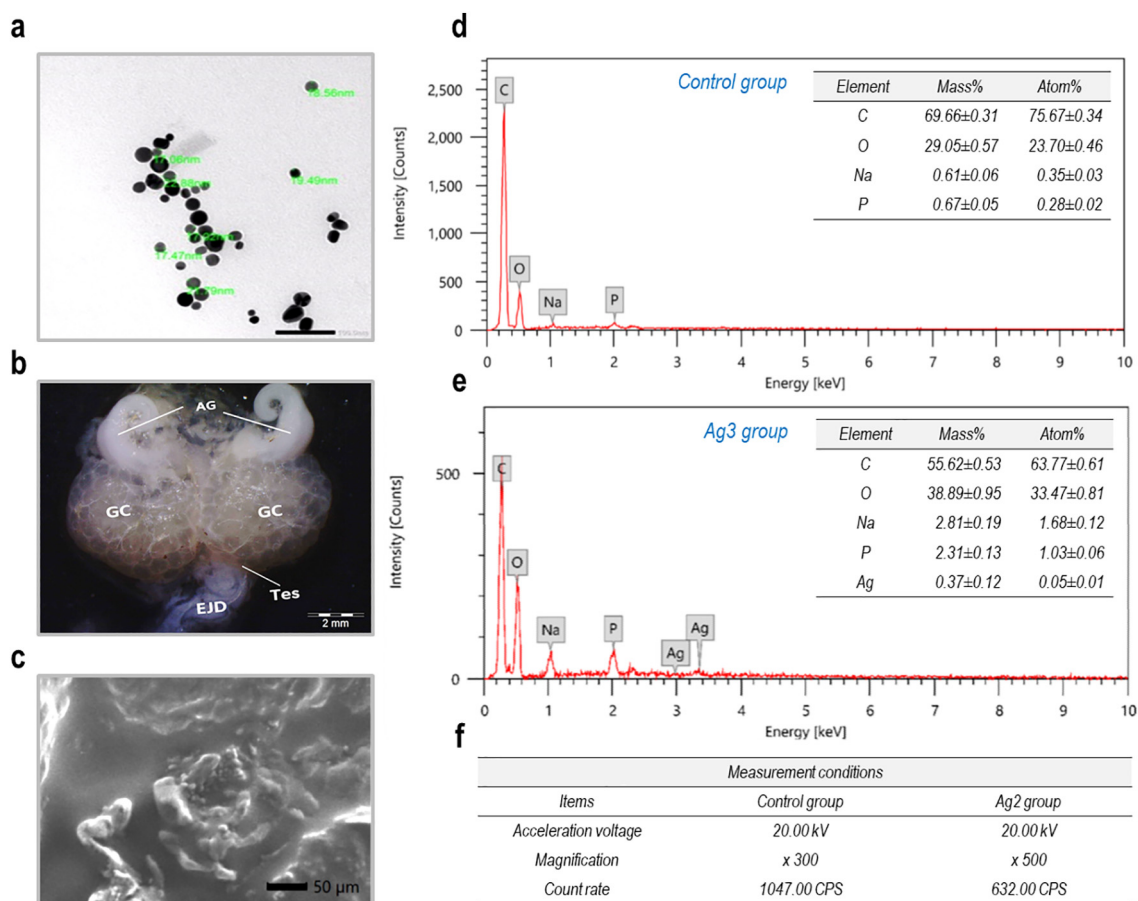
Fig. 2. Transmission Electron micrograph (TEM) of AgNPs (a). Male reproductive system of *Blaps polychresta* (b). Energy-dispersive X-ray (EDX) spectra of a selected area of the testis (c) - qualitative elemental composition, and quantitative analysis (insert in the graphs) in control (d) and Ag treated (e) groups; EDX measurement conditions (f).
Abbreviations: Testis (Tes); germinal cyst (GC); accessory gland (AG); ejaculatory duct (EJD). In Fig d and e: horizontal scale – X-ray energy; vertical scale – X-ray counts.

prepared for microscopic analysis. The tissue samples were frozen to −70 °C and lyophilized at −35 °C for 8 h. Then, the dried samples were stuck on aluminum supports with double-sided adhesive carbon tape. The last step was coating the sample surface with gold film (≥20 nm) to protect them against thermal damage and other adverse effects possibly occurring during electron beam work (Fischer et al., 2012). Then, the prepared slides were scanned by scanning electron microscopy (SEM; JEOL JSM-5300) with the settings shown in the table in Fig. 2f (at an accelerating voltage of 20 kV). Each peak was detected automatically by EDX software. The signal intensity was measured for each element in the sample (Fig. 2d–e). The same elements were analyzed in calibration standards of known composition. A stationary spot (X500) was examined at random for 110 s (El-Ashram et al., 2020).

2.6. Cell viability evaluation and DNA damage

Cell viability was measured using the Annexin V-FITC assay kit (Sigma–Aldrich, Germany) following the manufacturer's protocol. The cell suspension was obtained by gentle homogenization of tissue in PBS buffer (pH 7.4; 4 °C) (Koopman et al., 1994). The obtained cells were washed twice in PBS and resuspended in binding buffer. Then, the cell suspension in binding buffer (195 μL) was mixed with Annexin V-FITC conjugate reagent (5 μL) and incubated in darkness for 10 min. Finally, the cells were washed, resuspended in 190 μL binding buffer, and mixed with 10 μL propidium iodide solution. The fluorescence of the cells was determined immediately with flow cytometry (Becton Dickinson, Franklin Lakes, NJ, USA). For data analysis, CellQuest Pro software version 5.2.1, 2005 (BD Biosciences, San Jose, CA) was used.

DNA damage was detected by the comet assay under alkaline conditions, following the procedure of Singh et al. (1988). The suspension of testicular cells was obtained by gentle maceration of tissue in cold Hank's balanced salt solution containing 20 mM ethylenediaminetetraacetic acid (EDTA) and 10% dimethyl sulfoxide (DMSO). The Star Frost microscope slides were coated with 0.65% normal-melting agarose. The cell suspension was mixed with low-melting agarose (final concentration 0.65%) and spread onto slides. After agarose solidification (~20 min at 4 °C), the third layer of 0.65% low-melting agarose (120 mL) was placed on the top. The slides were immersed in lysis buffer (2.5 M NaCl, 100 mM EDTA, 10 mM Tris, 1% Triton X-100, 10% DMSO, pH 10.0) at 4 °C and left overnight to enable lysis of cell membranes. After washing (3×) in ultrapure water, the slides were immersed in electrophoresis buffer (1 mM EDTA, 300 mM NaOH, pH 13.0) and incubated for 20 min, and then electrophoresis was conducted for 20 min (at 300 mA). After electrophoresis, the slides were washed (3×) with 0.4 M Tris pH 7.5 for 15 min and dehydrated in 96% ethanol (~30 s). Before comet visualization, slides were rehydrated by immersion in ultrapure water (~5 min) and stained with ethidium bromide solution (20 mg/mL). The comets were scored using a fluorescence microscope (LEICA DMLS, 400× magnification). At each slide, 100 comets were examined.

2.7. Biochemical assays

To prepare the samples for enzymatic determinations, the testes were dissected on ice and washed three times in a normal saline solution (0.9%), slightly dried on tissue paper, weighed, and then homogenized (2 min) in Tris-HCl buffer (pH 7.4; tissue/buffer ratio 1:5). After

centrifugation (15,000 ×g; 4 °C, 60 min), the supernatant was gently decanted and stored at -70 °C until use. The following parameters were measured: protein content (PC) and malondialdehyde (MDA) concentration, as well as the activity of aspartate aminotransferase (AST), alanine aminotransferase (ALT), superoxide dismutase (SOD), catalase (CAT), glutathione peroxidase (GPx), and glutathione S-transferase (GST).

The total protein content was determined according to Lowry et al. (1951) using bovine serum albumin as a standard and expressed as mg/g tissue.

Determination of MDA content was carried out following Ohkawa et al. (1979). The principle of this method is the reaction of 2-thiobarbituric acid (TBA) with malondialdehyde, which produces a pink product, 2-thiobarbituric acid-reactive substance (TBARS). Briefly, the reaction mixture, containing supernatant, 8% sodium dodecyl sulfate, 20% acetic acid, 0.8% TBA and ultrapure water, at a proportion of 1:2:15:15:7 (v/v/v/v/v) was incubated at 95 °C for 1 h. After cooling, ultrapure water and a mixture of butanol-pyridine 15:1 (v/v) were added to the sample, followed by shaking for 10 min and centrifugation (15,000 ×g; 10 min). The absorbance of the upper layer (butanol-pyridine) was measured at 532 nm. After calculation, the MDA content in the samples was expressed as nmol/mg of tissue.

AST and ALT activities in the samples were measured with the use of commercial Biolabo (France) kits REFs 80025 and 80027, according to the manufacturer's protocols with a modification for insect material, as suggested by Łoś and Strachecka (2018). After mixing AST or ALT reagent with supernatant at a proportion of 10:1 (v/v), the samples were vortexed for ~3 s and incubated at 37 °C for 30 s. Then, the absorbance at 340 nm was measured. The results are expressed in U/mg protein.

SOD activity was measured according to Misra and Fridovich (1972). The method is based on monitoring the rate of adrenaline autooxidation. The absorbance of the reaction mixture, which contained the supernatant, sodium carbonate buffer (200 mM; pH 10.0), EDTA (10 mM), and freshly prepared epinephrine (15 mM), was measured at 480 nm. In the chart, SOD activity is expressed in mU/mg protein. The activity unit was defined as the amount of enzyme that inhibited 50% of the control reaction of adrenaline autooxidation per min.

CAT was measured following the method of Aebi (1984). During the reaction, the rate of decrease in the concentration of H_2O_2 in the sample was detected. The absorbance of the reaction mixture, containing the supernatant, phosphate buffer (50 mM, pH 7.0), and freshly prepared H_2O_2 (10 mM), was measured spectrophotometrically at a wavelength of 240 nm. CAT activity was expressed in mU/mg protein.

GPx activity was investigated using the method of Paglia and Valentine (1967). Cumene hydroperoxide (cumOOH) was used as a substrate. The reaction mixture contained the supernatant, 0.05 M phosphate buffer (pH 7.0), 1.25 mM EDTA, 1 mM sodium azide (NaN_3 - as the catalase inhibitor), 1 mM reduced glutathione (GSH), 1 IU of glutathione reductase, and 0.1 mM NADPH. The reaction was started by adding 0.2 mM cumOOH. Absorbance was measured spectrophotometrically at 340 nm over 2 min. Enzymatic activity was expressed in mU/mg protein.

GST activity was measured by the method described by Yu (1982) and Yu and Hsu (1993), with 1-chloro-2,4-dinitrobenzene (CDNB) as a substrate. The reaction mixture contained the supernatant, 33 mM Tris-HCl buffer (pH 9.0) and 7.5 mM GSH. The addition of 15 mM CDNB initiated the reaction. During the GST-catalyzed reaction, a complex of glutathione with CDNB was formed, the concentration of which was measured spectrophotometrically at a wavelength of 340 nm. The results were expressed as mU/mg protein.

2.8. Histological and ultrastructural analysis

For the histological study, testes, immediately after dissection, were fixed in 4% formaldehyde and 1% glutaraldehyde in a 0.1 M phosphate buffer (pH 7.2, 4 °C, 3 h). After postfixation in 2% osmium tetroxide (OsO_4) in phosphate buffer (pH 7.2, 2 h), the tissue was washed in the buffer and dehydrated at 4 °C in a graded concentration series of ethanol (50, 70, 90, 95, and 100% for 15 min each) and then embedded in an Epon–Araldite mixture. The semithin sections (1 mm thick) were stained with toluidine blue.

For the ultrastructure analysis, the tissues were fixed in 4F1G buffer (pH 7.2) containing 40% formaldehyde (10 mL), 50% glutaraldehyde (2 mL), monobasic sodium phosphate (1.16 mg), NaOH (0.27 mg), and ultrapure water (up to 100 mL). Then, the tissues were washed in 0.1 M phosphate buffer (2 h at 4 °C), postfixed in 1% OsO_4 (2 h at 4 °C), and washed 3× for 10 min. After dehydration in a graded concentration series of ethanol, the samples were filtered in propylene oxide and embedded in the Araldite-Epon mixture. Ultrathin sections (70 nm) were cut on an LKB ultramicrotome with a glass knife, fixed on copper grids, and stained with uranyl acetate and lead citrate (Reynolds, 1963). Finally, the slides were examined with a JEOL 100CX Electron Microscope at 80 kV.

2.9. Statistical procedures

Mortality curves were determined for all study groups using Kaplan–Meier survival analysis. The significance of differences between all curves was calculated using the log-rank test (Chi2, p < 0.05) for multitrial comparisons. Multiple curve comparisons (pairwise) were performed using the log-rank test (after applying the Bonferroni correction) to identify potential differences between closely spaced curves. Four groups were compared at FWER (familywise error rate) = 0.008. Data on the viability of the cells (Annexin V-FITC apoptosis test results) and data from biochemical analyses were assessed for normality using the Kolmogorov–Smirnov and Lilliefors tests. Since some of the data did not meet the assumption of normal distribution, we decided to analyze all data using the nonparametric Mann–Whitney U test (p > 0.05). Survival time was calculated for the 20 animals in each group. Other parameters were assessed for 3–5 individuals per group. All statistical analyses were performed using Statistica 13.3 software.

3. Results

3.1. B. polychresta survival after AgNPs application

The curves in Fig. 1 show the expected survival time of *B. polychresta* after a single application of AgNPs on the day of starting the experiment (Day 0) and cover a period of 30 days of observation. Kaplan–Meier survival analysis revealed an adverse effect of AgNPs on insect survival, dependent on the dose of nanoparticles (Fig. 1b–c). The log-rank test, performed for all groups together, confirmed the highly significant effect of the injection of nanoparticles (Chi2 = 93.11, p < 0.0001; Fig. 1c). However, only the group treated with the highest AgNP dose (Ag7 group) revealed 100% mortality. The Ag5 group revealed cumulative mortality at Day 30 of 50%. Thus, this dose can be considered the LD50 for *B. polychresta* 30 days after the application of AgNPs. Comparison of the survival curves with the log-rank test, considering the 4 groups treated with lower doses (Ag2-Ag5 groups), revealed no significant differences between these groups (Chi2 = 7.02, p = 0.0713; Fig. 1c). Further analysis, performed in pairs in the groups showing mortality between 10% and 50%, revealed a significant difference in the survival probability only between the Ag2 and Ag5 groups (Chi2 = −2.63, p = 0.0084; Fig. 1c). Pairwise comparison of the control and Ag1 groups was not possible due to fewer than 2 complete observations, i.e., death. The Ag2 group was the first for which a pairwise log-rank analysis could be performed and thus accepted the null hypothesis of no difference between this group and the control group. Subsequent groups (receiving increasingly higher doses) differed significantly in their survival time compared to the control group. On this basis, it was decided to carry out further biochemical and histological analyses on the beetles from the Ag3 group, considering the dose of 0.03 mg AgNPs/g b.w.t. as the LOAEL.

3.2. Content of selected elements in the testis of B. polychresta

EDX revealed the presence of four basic elements in the testes of males of the control and Ag3 groups, namely, C, O, Na, and P. The percentage of the elements is shown in Fig. 2d–e. No peak characteristic of silver was detected in the tissue of insects from the control group. In contrast, in insects subjected to a single injection of AgNPs at a dose of 0.03 mg/g b.w.t., Ag was found in the testes after 30 days. The mean percentage of Ag in this tissue was 0.37 ± 0.12.

3.3. Cell viability and DNA damage in testicular cells of B. polychresta

The single application of AgNPs at a dose of 0.03 mg/g b.w.t. had a significant effect on the viability of cells isolated from male testes (Fig. 3a–c). Annexin V-FITC assay revealed a significantly lower share of viable cells in the Ag3 group compared to insects from the control group, where the number of viable cells was 80%. For comparison, the viable cell count in the Ag3 group was only slightly above 45%. There were also significant differences between the two groups in the percentage of cells with necrosis and apoptosis. Interestingly, in insects from the Ag3 group, the share of necrotic cells decreased significantly, while the share of apoptotic cells increased compared to control insects. Necrosis was found in 13.7% of control insect cells and only in 4.9% of insect testicular cells exposed to AgNPs. Cells in the early apoptotic phase accounted for as much as 32.8% of the testes of Ag3 insects, while for insects from the control group, this value was only 6.3%. Late apoptosis was the state relatively least frequently observed; in the control group, the median for this type of cell was only 0.82%, and for the Ag3 group, the value was 16.2%. The differences described above were statistically significant (Mann–Whitney U test; $p < 0.05$; Fig. 3a–c).
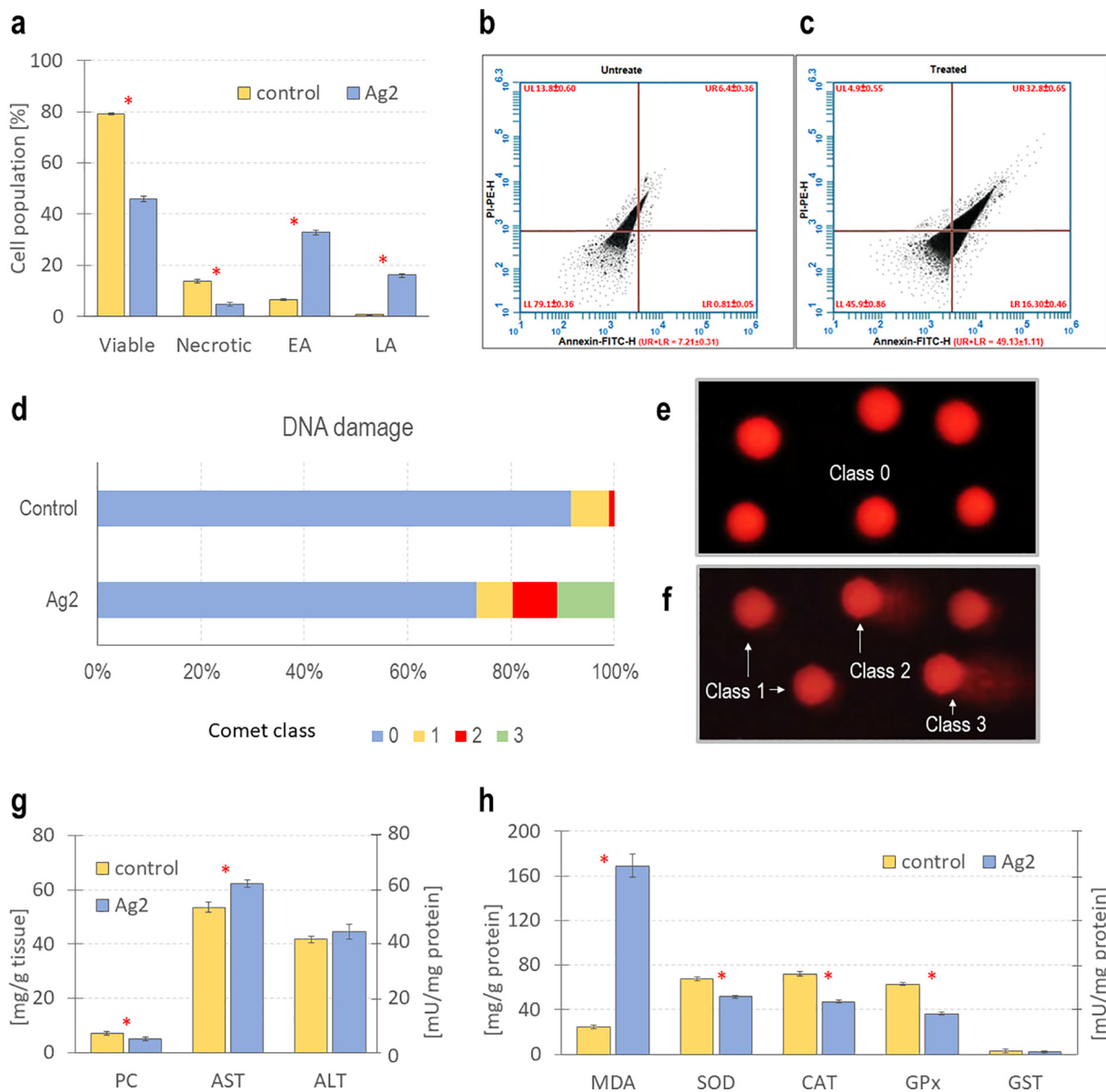

Fig. 3. Flow cytometry analysis of Annexin-V-FITC and propidium iodide staining of *Blaps polychresta* testis tissue (a), and plots for control (b) and Ag treated (c) groups. DNA damage using the comet assay (d) in the testis of beetles from control (e) Ag treated (f) groups. Mean ± SE concentration of protein and activity of enzymes involved in protein transformation - AST and ALT (g), MDA concentration, and activity of antioxidant enzymes (h) in beetle testis. Abbreviations: Necrotic cells – the upper left (UL) quadrant (PI+/Annexin V−); Viable cells – the left lower (LL) quadrant (PI−/Annexin V−); Early apoptotic cells (EA) – the upper right (UR) quadrant (PI+/Annexin V+); Late apoptotic cells (LA) – the lower right (LR) quadrant (PI−/Annexin V+); Class 0–3 – reflecting the degree of DNA damage: 0 – no damage, 3 – the greatest damage; Protein content (PC); Aspartate aminotransferase (AST); Alanine aminotransferase (ALT); Malondialdehyde (MDA); Superoxide dismutase (SOD); Catalase (CAT); Glutathione peroxidase (GPx); Glutathione S-transferase (GST). The red star above bars – significant differences between control and treated groups (Mann–Whitney U test, $p < 0.05$).

The comet assay also revealed a significant effect of AgNPs at selected doses on the nuclei of *B. polychresta* testicular cells. Despite a long time since injection, the number of nuclei with damaged DNA was significantly greater in the Ag3 group. The number of nuclei without evidence of DNA damage in individuals from the control group was slightly over 91%. The remaining cells (8.3%) were classified in the first (7.3%) or second (1.0%) DNA damage class. Moreover, in the cells of the control insects, practically no nuclei with damage typical of the third class were found. However, the percentage of cell nuclei without damage in beetles injected with AgNPs was 73.3%. The remaining cells (26.7%) presented different degrees of damage: 7.0% in the first class, 8.7% in the second, and 11.0% in the third (Fig. 3d–f).

3.4. The level of stress markers in B. polychresta after AgNP application

The single application of AgNPs to beetles at a dose of 0.03 mg/g body weight resulted in changes in the protein content and part of the stress markers measured after 30 days of exposure. Significantly lower protein content was found in the group treated with AgNPs compared to the control group. The activity of AST in the testes of insects from the Ag3 group was significantly higher than the activity of AST in the testes of insects in the control group. However, ALT activity did not differ between the groups studied (Fig. 3g). Importantly, AgNPs caused a visible highly significant increase in MDA content compared to the MDA content in the control group. The concentrations of MDA in the testes from Ag3-treated males were almost seven times higher than the value determined for the control group. On Day 30 after AgNP injection, the activity of enzymes responsible for removing reactive oxygen species (ROS), namely, SOD, CAT, and GPx, was significantly lower in

the Ag3 group than in the control group. GST activity was low and did not differ between the groups studied (Fig. 3h).

3.5. Testicular micro- and ultrastructure of B. polychresta

Analysis of histological cross-sections through adult *B. polychresta* testes from the control group revealed a typical tissue structure, with visible male germ cells (spermatogonia, spermatocytes, spermatids) without visible damage or lesions (Fig. 4a–f). Microscopic examination of testes of the AgNP-treated group revealed a series of anomalies in the gonadal structure of male *B. polychresta*. Rupture of the cyst wall and a series of damage to the germ cells were observed in the form of morphologically altered spermatogonia and spermatocytes as well as necrotic spermatids (Fig. 4a′–f′).

TEM analysis of gonads of control males revealed a normal spermatogenesis process (Figs. 5a–d and 6a–c). Regular spermatogonia, primary spermatocytes with synaptonemal complexes, each with a nucleus having normal chromatin condensation, a regular nuclear envelope, and the cytoplasm having numerous mitochondria were observed. Secondary spermatocytes had a smaller nucleus than primary spermatocytes, and the cytoplasm had numerous mitochondria. Each early spermatid was characterized by a normal peripherally located nucleus, mitochondrial nebenkern, and a Golgi body (Fig. 5a–d). Late spermatids were characterized in testes from the control group by the presence of a nucleus having a nuclear envelope, mitochondria - separated into two mitochondrial derivatives, accessory bodies, and flagella - each of which had an axoneme and two small, round accessory bodies (Fig. 6a–c). In addition, the head region of the sperm in testes from the control group had a normal, oval nucleus with a nuclear envelope and an apical acrosome. Flagella of normal sperm showed two symmetrical, fully formed
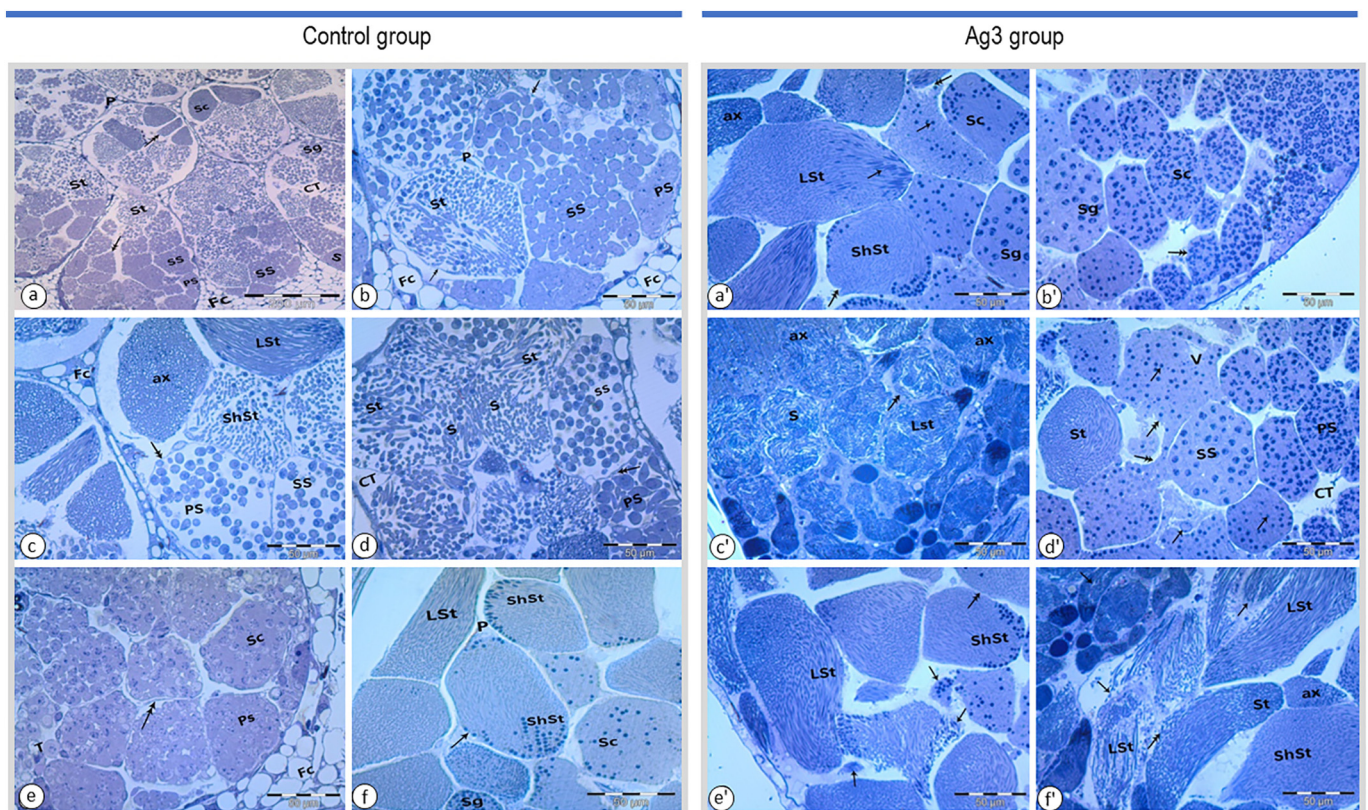

Fig. 4. Semithin section of testicular follicles of *B. polychresta* from control (a–f) and Ag treated (a′–f′) groups.
Abbreviations: Spermatogonia (Sg); Spermatocytes (Sc); Primary spermatocytes (PS); Secondary spermatocytes (SS); Spermatid (St); Short spermatids (Shst); Long spermatids (LSt); Spermatozoa (S), Axoneme (ax); Parietal cells (P); Fat cells (Fc); Connective tissue (CT); Trachea (T).
Figs. a–f: Epithelial wall (arrow); Cyst wall (double head arrow). Figs. a′–f′: a′ - necrotic Spermatids; b′ – morphologically altered Spermatogonia and Spermatocytes; c′ – necrotic Spermatids and Spermatozoa; d′–f′ – necrotic short and/or long Spermatids; Rupture of cyst wall (double head arrow); Necrotic spermatids/spermatozoa (arrow).
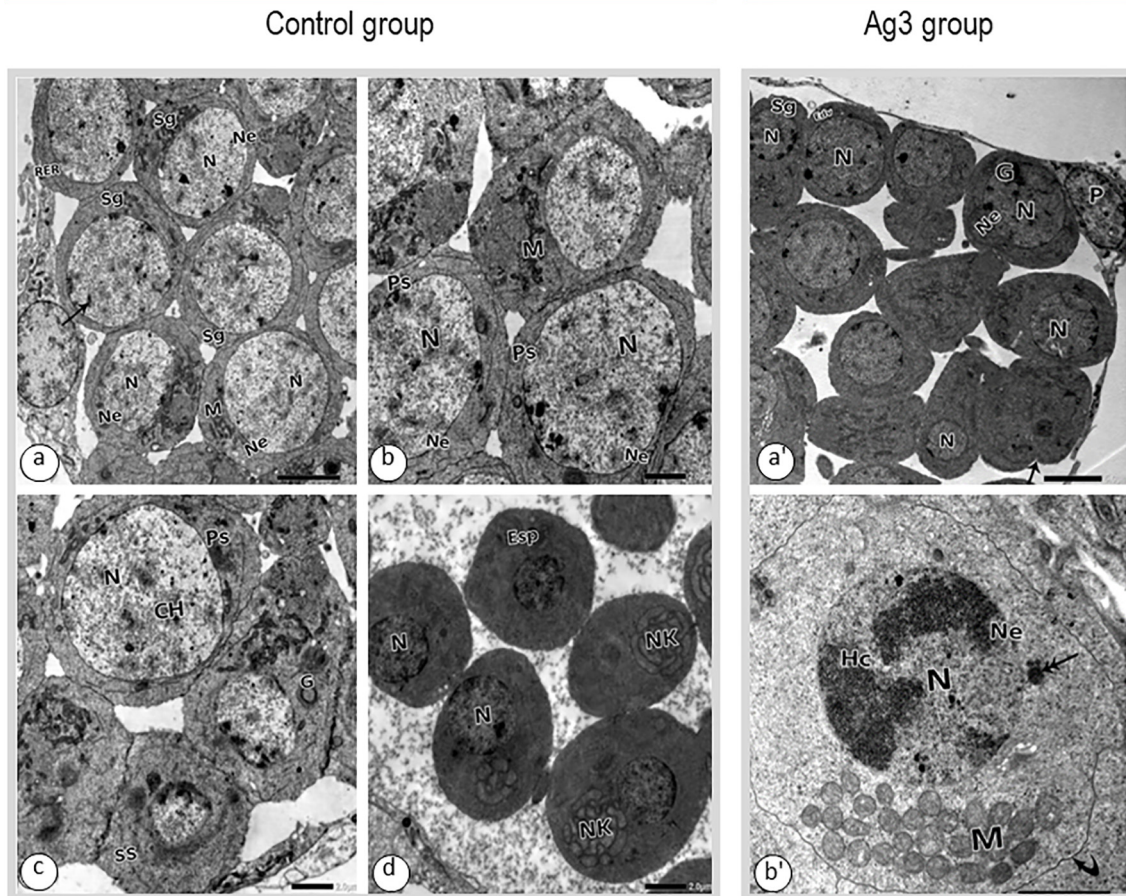
Fig. 5. Transmission electron micrograph in normal (a–d; control group) and abnormal (a′–b′; Ag treated group) spermatogenesis of *B. polychresta*.
Abbreviations: Spermatogonia (Sg); Primary spermatocyte (PS); secondary spermatocyte (SS); early spermatids (Esp); parietal cells (P); nucleus (N); chromatin (CH); hetero chromatin (Hc); nuclear envelope (Ne); electron dense vesicle (Edv); mitochondria (M); mitochondrial nebenkern (NK), Golgi body (G).
a - Spermatogonia; b - primary spermatocyte with synaptonemal complexes (arrow); c - secondary spermatocyte; d - early spermatids; a′ – Sg cells with two nuclei in the same cytoplasm, deformed cells with irregular cyst wall (arrow); b′ – deformed primary spermatocytes with irregular shape (curved arrow), dense bodies (double head arrow).

mitochondrial derivatives, two small accessory bodies, and an axoneme (Fig. 7a–f). However, the AgNP-treated group showed abnormal spermatogenesis. In the micrographs, deformed cells with irregular cyst walls were present. Some spermatogonia were characterized by the presence of two nuclei in the same cytoplasm and electron-dense vesicles. Additionally, deformed primary spermatocytes were observed. The most common abnormalities were an irregular cell shape, degenerated mitochondria, and dense bodies in the cell (Fig. 5a′–b′). Early spermatids showed abnormal cell structure. Some of these cells were deformed and characterized as having a peripheral nucleus, electron-dense vesicles, and vacuolated cytoplasm. Flagella of late spermatids possessed malformed or degenerated mitochondrial derivatives, disrupted chromatin, and residual and/or highly vacuolated cytoplasm. Agglutinated spermatids with degenerated axonemes and deformed abnormal mitochondrial derivatives were observed. Moreover, some of the late spermatids had abnormal head morphology. Parietal cells possessed a nucleus with an irregular nuclear envelope and mitochondria with dense bodies. Some of the cells had enlarged cytoplasm and dense vesicles (Figs. 6a′–f′ and 7a′–d′).

The analysis of the nuclei using SEM confirmed the negative influence of AgNPs on the spermatogenesis process in *B. polychresta*. The sperm of insects from the control group showed normal structure (Fig. 8a–d). However, SEM analysis of AgNP-treated individuals revealed the presence of agglutinated spermatids (tail to tail or head to head), some of which had head sutures (Fig. 8a–d′).

4. Discussion

The increasing phenomenon of AgNP penetration into ecosystems is now considered an undeniable fact. The migration routes of AgNPs and general aspects of AgNP toxicity for various organisms, mainly model organisms, have been described. Potential risks to humans and the environment have also been estimated (Tortella et al., 2020). However, the impact of AgNPs on wild organisms, especially terrestrial organisms, is still poorly known. A relationship between AgNP dose and mortality has been described for several model organisms, such as *Drosophila melanogaster* (Raj et al., 2017) and *Caenorhabditis elegans*, or a few earthworm species (Tortella et al., 2020). In our studies, we assessed the mortality of *B. porchresta* at a series of doses (Fig. 1b–c). Taking mortality as an endpoint, a dose of 0.01 mg/g body weight can be considered a no observed effect level (NOEL) for mortality; a dose of 0.02 can be considered the lowest observed effect level (LOEL), and a dose of 0.03 can be considered the LOAEL. Interestingly, a dose less than twice the LOAEL (namely, 0.05 mg/g body weight) resulted in 50% beetle death (LD50/30) 30 days after exposure. In comparison, for mice, the LD50 (14 days after injection of AgNPs) has been reported to be 250 and 350 mg/kg body weight, depending on the size of the AgNPs (Hoseini-Alfatemi et al., 2020). These values are approximately 5–7 times higher than those found in our experiment. Thus, presumably, *B. polychresta* is much more sensitive to AgNPs than mice and possibly other mammals, even considering the shorter monitoring period of mouse survival.
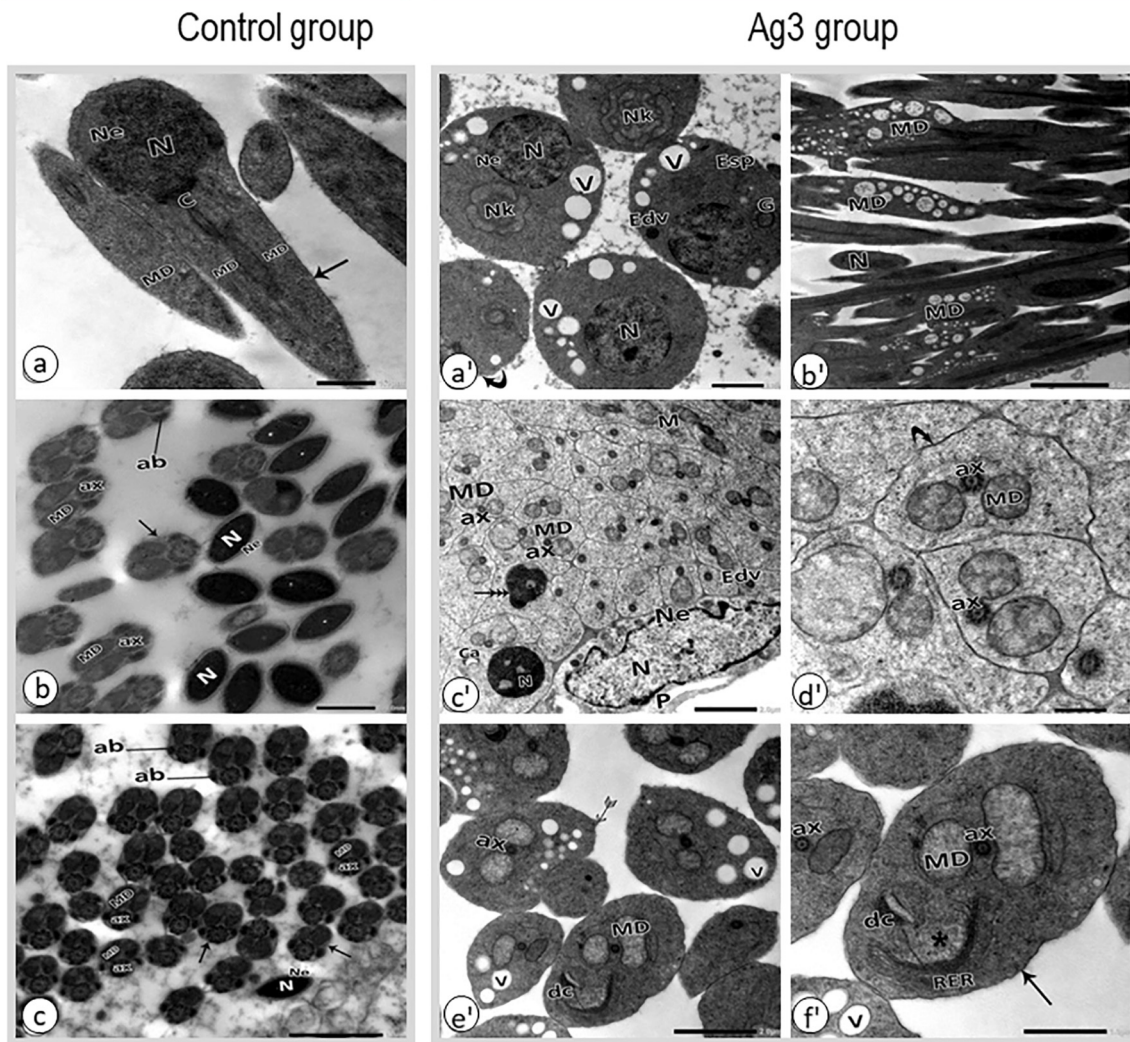
Fig. 6. Transmission electron micrograph in normal (a–c; control group) and abnormal (a′–f′; Ag treated group) spermatogenesis of *B. polychresta*.
Abbreviations: early spermatids (Esp); parietal cell (P); nucleus (N), nuclear envelope (Ne), mitochondrial derivatives (MD); mitochondrial nebenkern (Nk); centriole (C), vacuolated cytoplasm (V); accessory body (ab); electron dense vesicle (Edv); Golgi body (G); axoneme (ax); dense bodies (Ca); residual cytoplasm (*); disrupted chromatin (dc), rough endoplasmic reticulum (RER).
a – longitudinal section of late spermatid with mitochondria and centriole; b – section in a normal late spermatid showing the two mitochondrial derivatives, a longitudinal nucleus could be observed with the nuclear envelope, accessory body, and axoneme; cross section in the head region of normal late spermatid, each with a nucleus; c – cross section in the head region of normal late spermatids, and cross section in the flagella; a′ – abnormal late spermatogenesis, abnormal early spermatids, each with peripheral nucleus, mitochondrial nebenkern, electron dense vesicle, Golgi body and with vacuolated cytoplasm; b′ – cross section in abnormal flagella of late spermatids with degenerated mitochondrial derivatives and highly vacuolated cytoplasm; c′ –a cross section showing parietal cell with a nucleus, irregular nuclear envelope and mitochondria with dense bodies, some cells with enlarged cytoplasm (three head arrow) with dense vesicle; d′ – agglutinated spermatids observed with degenerated axoneme, deformed abnormal mitochondrial derivatives, deformed cell (curved arrow); e′ – abnormal spermatogenesis showing cross section in abnormal flagella of late spermatids with malformed mitochondrial derivatives, highly vacuolated cytoplasm and abnormal head morphology of spermatids (spear arrow); f′ – magnified cross section in the flagella of late spermatids showing residual cytoplasm, disrupted chromatin, rough endoplasmic reticulum and axoneme.

Shortening of survival time was accompanied by disturbances at the tissue, cellular and molecular marker levels, which are presented in Figs. 3–8. DNA damage measured by the comet assay is one of the commonly used and valued markers of genotoxicity due to its simplicity and ease of evaluation (Collins, 2004; Dhawan et al., 2009; Gajski et al., 2019a, 2019b). Its usefulness has been confirmed many times in studies on insects exposed to various stress factors, including nanoparticles (Augustyniak et al., 2016a; Karpeta-Kaczmarek et al., 2016; Fang et al., 2021; Kheirallah et al., 2021). However, this marker requires careful interpretation, also considering exposure time. Its use as a marker works well in the case of short-term exposure to relatively high doses. Chronic exposure to sublethal doses (in the NOEL or LOEL range) should strengthen the antioxidant shield and intensify the processes of fast repair of damage. DNA is a crucial material of priority importance for an individual and species. Thus, after a single exposure to a low dose, a

temporary increase in DNA damage can be expected, which, however, should be repaired rapidly (Augustyniak et al., 2014, 2015; Augustyniak et al., 2016b; Dexheimer, 2013; Augustyniak et al., 2020; Flasz et al., 2021). Nevertheless, in our study, 30 days after exposure, DNA damage in the Ag3 group was still significantly greater than the DN A damage in the control group (Fig. 3d–f). A logical explanation for this result is the internalization of AgNPs into the testes of males. The deposited AgNPs can then act as a source of silver ions (McShan et al., 2014), causing chronic redox imbalances and participating in the free radical cascade over a long time after a single exposure. Free radicals are one of the causes of DNA damage increases. Consistent with this concept is the drastic increase in MDA concentrations in the gonads of Ag3 males (Fig. 3h). MDA is the most studied marker of lipid peroxidation (Gil et al., 2002; Cepoi et al., 2020). MDA is highly toxic. It can interact with DNA and proteins, causing damage to these molecules (Del Rio et al., 2005). The
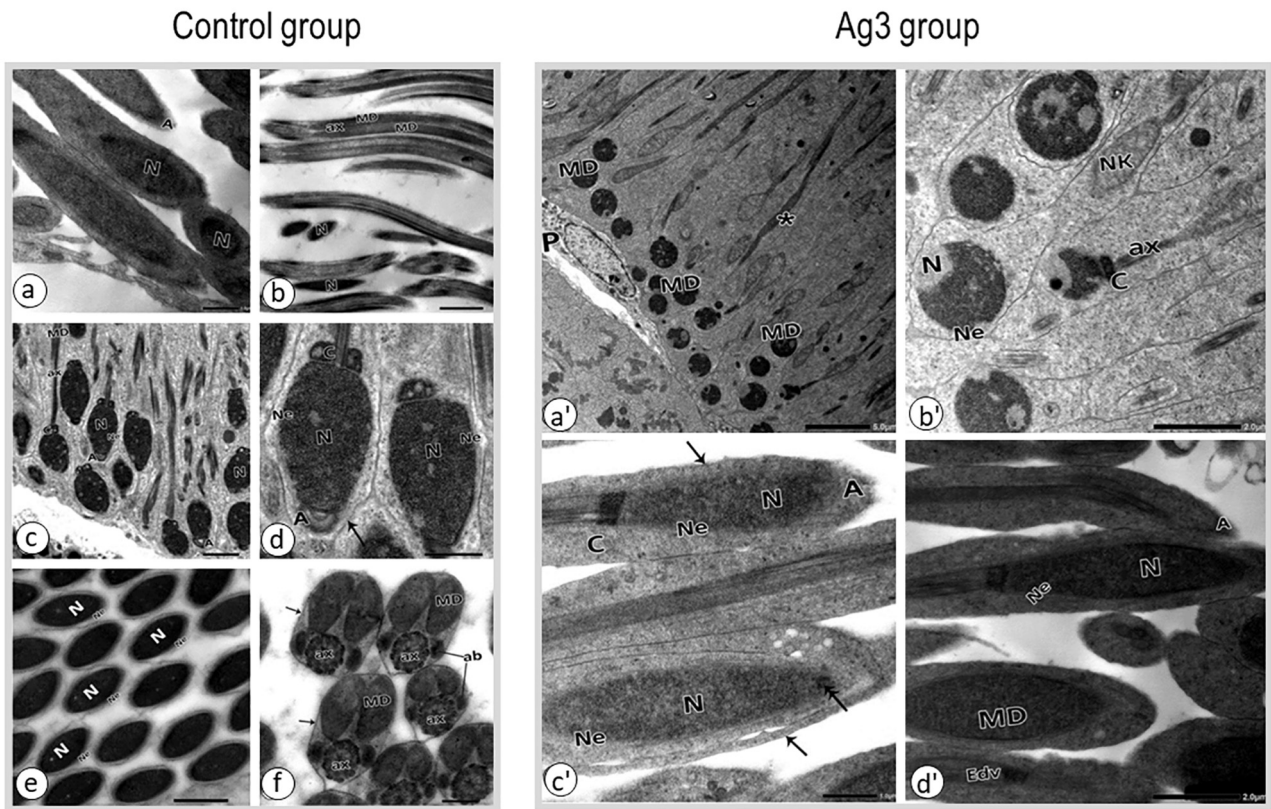
Fig. 7. Transmission electron micrograph in normal (a–f; control group) and abnormal (a′–d′; Ag treated group) spermatogenesis of *B. polychresta*.
Abbreviations: nucleus (N); nuclear envelope (Ne); apical acrosome (A); mitochondrial derivatives (MD); mitochondrial nebenkern (NK); axoneme (ax); centriole (C); accessory bodies (ab); residual cytoplasm (*); mitochondrial derivatives (MD); parietal cell (P); electron dense vesicle (Edv), acrosome (A).
a – a longitudinal section in the head region of a normal sperm with a nucleus and an apical acrosome; b – longitudinal section in the flagella of normal sperm showing two mitochondrial derivatives and axoneme; c – longitudinal section showing head and flagella of normal sperm; d – magnified micrograph showing the head region with the apical acrosome and centriole; e – higher magnification of cross section in the head region of normal sperms, each with an oval nucleus with nuclear envelope; f – cross section in the flagella of normal sperms, each having an axoneme, two symmetrical fully formed mitochondrial derivatives and two small accessory bodies; a′ – spermatids with residual cytoplasm, deformed mitochondrial derivatives and parietal cell; b′ – spermatids with irregular nuclear envelope, nucleus, centriole, axoneme and degenerated nebenkern; c′–d′ – convoluted plasma membrane (arrow), electron dense vesicle, centriole, dense bodies (double head arrow) and acrosome.
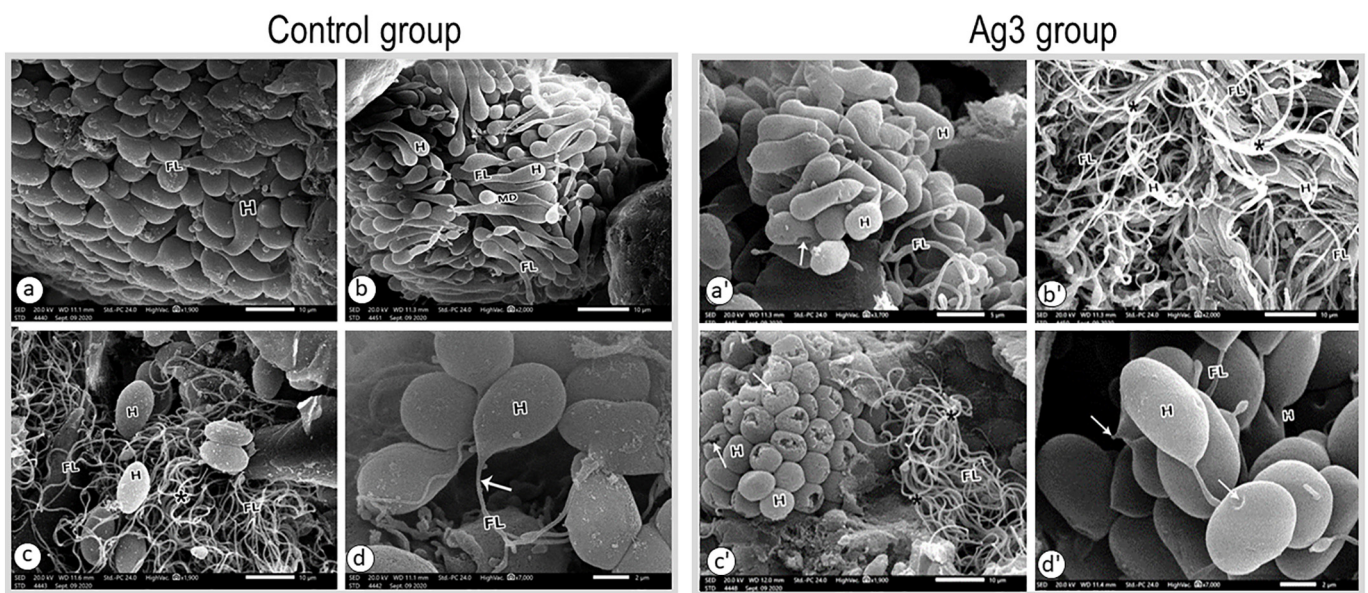

Fig. 8. SEM of the testicular follicles of *B. polychresta* from the control (a-d) and Ag treated (a′–d′) groups.
Abbreviations: head (H); flagellum (FL); mitochondrial derivatives (MD).
c–d – late spermatids, suture in the plasma membrane (*), axoneme (arrow). a′–d′ – agglutinated spermatids with head sutures (arrow) and tail to tail (*).

genotoxic potential of this aldehyde is most likely partly responsible for the increase in DNA damage in *B. polychresta* from the Ag3 group. A similar relationship between exposure to nickel oxide nanoparticles (NiO-NPs) and the degree of DNA damage in the ovaries was demonstrated for *B. polychresta* females subjected to a single injection (Kheirallah et al., 2021). However, the level of MDA was not measured in the study mentioned. Dose-dependent DNA damage, accompanied by an increase in MDA concentration, was also demonstrated for sperm of Wistar rats chronically exposed to zinc oxide nanoparticles (Husain et al., 2019). Thus, it can be generalized that the phenomena are typical for metal nanoparticles and occur in both invertebrates and vertebrates, as long as the nanoparticles are internalized in gonads.

Complementing the described relationships is the reduction in the protein content observed in Ag3 beetles (Fig. 3g), including enzymatic proteins that play a key role in eliminating the effects of oxidative stress (Fig. 3h). SOD (responsible for the dismutation of the superoxide radical anion), CAT (decomposing hydrogen peroxide), and GPx (reducing hydrogen peroxide and organic peroxides) should intensify activity under oxidative stress (Yousef et al., 2019). However, prolonged stress may result in the depletion of energy resources and impairment of enzyme activity and the synthesis of new molecules (El-Gendy et al., 2020). Fang et al. (2021), investigating the ovarian cell line BmN of *Bombyx mori*, showed that exposure to titanium dioxide nanoparticles (TiO$_2$NPs) leads to reduced transcription of antioxidant genes, accumulation of peroxides, and inflammation. Energy reserves can be allocated toward other enzyme pathways, for example, ALT and/or AST. Both enzymes may perform slightly different functions in insects than in mammals, but they can still be used to assess the immunity status (Łoś and Strachecka, 2018). ALT and AST activity in bees may increase with aging but decrease after contact with unfavorable or harmful factors. At a low dose, cyromazine reduced ALT and AST in *Culex pipiens*, while a higher dose caused the opposite effect (Assar et al., 2012). Additionally, the administration of cytotoxic drugs increased ALT activity in *Bombyx mori* (Inagaki et al., 2012). In our experiment, the ALT and AST activities were significantly higher in the Ag3 group than in the control group (Fig. 3g). Łoś and Strachecka (2018) pointed out that ALT and AST, markers used in assessing liver function in mammals, can also be used as markers of pathological changes in insects. Importantly, great caution is advised, as these enzymes may have a slightly different function for particular insect species (Łoś and Strachecka, 2018).

The above-described effects of AgNPs are reflected in the condition of cells and tissues. In insects treated with AgNPs at a dose of 0.03 mg/g b.w., there was a significant reduction in viable cells and an increase in the number of apoptotic cells, especially early apoptosis (Fig. 3a). Similar results were reported by El-Ashram et al. (2020) in *Trachyderma hispida* ovaries after exposure to gold nanoparticles (Au-NPs) and by Kheirallah et al. (2021) in *B. polychresta* ovaries injected with NiO-NPs. Additionally, O'Donnell et al. (2017) revealed an increase in apoptosis in germ cells of *Caenorhabditis elegans* treated with zinc oxide nanoparticles (ZnONPs). Increased apoptosis, a process of programmed and controlled cell death, attempts to maintain homeostasis and indirectly indicate an increase in abnormalities in cells exposed to metal nanoparticles, including AgNPs. Interestingly, *B. polychresta* from the Ag3 group showed significantly lower necrosis than insects from the control group. Apoptosis and necrosis are types of cell death that differ in their genesis and course (Krysko et al., 2008; Kanduc et al., 2002). Necrosis can be caused by a variety of factors, including bacterial infections. Necrosis is regulated at the cell level in the context of host-pathogen interactions and may be involved in (but may also contribute to) infection (Blériot and Lecuit, 2016). Both apoptosis and necrosis in spermatozoa have been observed following in vitro treatment of sperm with pathogenic bacteria (Fraczek et al., 2015). Considering the antiseptic nature of AgNPs, we can hypothesize that AgNPs offer a chance to reduce the risk of infection and inflammation in various compartments of the animal's body. This, in turn, can lower the risk of necrosis. *B. polychresta* is a terrestrial insect that lives in contact with various microorganisms present in the soil. Some of them can contribute to inflammation and accelerate necrosis. AgNPs can limit the number of such bacteria and their adverse effects on *B. polychresta*. This somewhat brave hypothesis requires further sophisticated research, which our team intends to perform in the future. Wang et al. (2018), discussing the potential adverse effects of NPs on the reproductive system, mentioned that AgNPs may be considered one of the most toxic. Detailed analysis of the structure and ultrastructure of the testes of male *B. polychresta* from the Ag3 group revealed many unfavorable changes (Figs. 4–8), which indicate severe degeneration of this organ. Changes in the structure and ultrastructure of the ovaries have been reported in *B. polychresta* after injection with NiO-NPs (Kheirallah et al., 2021) and in *T. hispida* ovaries exposed to Au-NPs (El-Ashram et al., 2020). Raj et al. (2017) showed that AgNPs significantly affect egg-laying capacity and impair ovarian growth. TiO$_2$NPs at high doses have shown reproductive toxicity to *B. mori* (Ni et al., 2015). Interestingly, however, low doses can enhance the reproduction and fecundity of *B. mori*, manifested by faster ovarian and testicular development and faster gamete formation and differentiation (Ni et al., 2015). This result highlights the importance of the dose. For beneficial (breeding) insects, it may be advisable to stimulate reproduction, in contrast to crop pests or disease vectors. However, it should be emphasized that any reproductive disorders are not advisable in wild insects.

5. Conclusions

This research describes the effects of the widely and readily used AgNPs on the testes of wild insects - *B. polychresta*. Even after a single application, AgNPs caused long-term effects manifested by numerous changes in the testes of male *B. polychresta*. Most likely, AgNPs, in a single exposure, take the form of chronic exposure, as the nanoparticles serve as the source of Ag ions in the animal's body. The long-term consequences of damage to the testes of wild animals, which may be associated with an increase in the mortality of individuals, extinction of species, and disturbance of the structure of ecosystems, should be emphasized. Therefore, considering the results of this study, we can reject the null hypothesis (H0) and accept the alternative hypothesis (H1). It is advisable to develop the principles of safe production, controlled use, and disposal of AgNPs.

CRediT authorship contribution statement

Lamia M. El-Samad: Conceptualization, Project administration, Validation, Formal analysis, Investigation, Supervision, Reviewing and editing the draft. **Saeed El-Ashramb:**. Project administration, Validation, Formal analysis, Supervision, Revising the draft. **Hussein K. Hussein:** Project administration, Validation, Formal analysis, Supervision, Revising the draft. **Karolin K. Abdul-Aziz:** Validation, Supervision, Revising the draft. **Eman H. Radwan:** Validation, Supervision, Revising the draft. **Nahed R. Bakr:** Methodology, Data curation, Formal analysis, Investigation, Writing - original draft. **Abeer ElWakil:** Validation, Formal analysis, Reviewing and editing the draft. **Maria Augustyniak:** Validation, Formal statistical analysis, Writing - original draft, Reviewing and editing the draft.

Declaration of competing interest

The authors declare that they have no known competing financial interests or personal relationships that could have appeared to influence the work reported in this paper.

References

Aebi, H., 1984. Catalase in vitro. Methods Enzymol. 105, 121–126. https://doi.org/10.1016/s0076-6879(84)05016-3.

Assar, A.A., Abo-El-Mahasen, M.M., Harba, N.M., Rady, A.A., 2012. Biochemical effects of cyromazine on Culex pipiens larvae (Dipter: Culicidae). J. Am. Sci. 8, 443–450.

Augustyniak, M., Orzechowska, H., Kędziorski, A., Sawczyn, T., Doleżych, B., 2014. DNA damage in grasshoppers' larvae - comet assay in environmental approach. Chemosphere 96, 180–187. https://doi.org/10.1016/j.chemosphere.2013.10.033.

Augustyniak, M., Nocoń, Ł., Kędziorski, A., Łaszczyca, P., Sawczyn, T., Tarnawska, M., Zawisza-Raszka, A., 2015. DNA damage in grasshopper Chorthippus brunneus (Orthoptera) hatchlings following paraquat exposure. Chemosphere 125, 212–219. https://doi.org/10.1016/j.chemosphere.2014.12.069.

Augustyniak, M., Gladysz, M., Dziewięcka, M., 2016a. The comet assay in insects - status, prospects and benefits for science. Rev. Mutat. Res. 767, 67–76. https://doi.org/10.1016/j.mrrev.2015.09.001.

Augustyniak, M., Płachetka-Bożek, A., Kafel, A., Babczyńska, A., Tarnawska, M., Janiak, A., Loba, A., Dziewięcka, M., Karpeta-Kaczmarek, J., Zawisza-Raszka, A., 2016b. Phenotypic plasticity, epigenetic or genetic modifications in relation to the duration of cd-exposure within a microevolution time range in the beet armyworm. PLoS One 11, e0167371. https://doi.org/10.1371/journal.pone.0167371.

Augustyniak, M., Tarnawska, M., Dziewięcka, M., Kafel, A., Rost-Roszkowska, M., Babczyńska, A., 2020. DNA damage in Spodoptera exigua after multigenerational cadmium exposure - a trade-off between genome stability and adaptation. Sci. Total Environ. 745, 141048. https://doi.org/10.1016/j.scitotenv.2020.141048.

Bhargava, A., Dev, A., Mohanbhai, S.J., Pareek, V., Jain, N., Choudhury, S.R., Panwar, J., Karmakar, S., 2021. Pre-coating of protein modulate patterns of corona formation, physiological stability and cytotoxicity of silver nanoparticles. Sci. Total Environ. 772, 144797. https://doi.org/10.1016/j.scitotenv.2020.144797.

Blériot, C., Lecuit, M., 2016. The interplay between regulated necrosis and bacterial infection. Cell. Mol. Life Sci. 73, 2369–2378. https://doi.org/10.1007/s00018-016-2206-1.

Cepoi, L., Rudi, L., Chiriac, T., Miscu, V., Rudic, V., 2020. Malondialdehyde - a potential marker of nanoparticle toxicity in an aquatic environment. One Health Risk Manag. 1 (1), 64–71. https://doi.org/10.38045/ohrm.2020.1.10.

Collins, A.R., 2004. The comet assay for DNA damage and repair: principles, applications, and limitations. Mol. Biotechnol. 26, 249–261. https://doi.org/10.1385/MB:26:3:249.

Dang, F., Huang, Y., Wang, Y., Zhou, D., Xing, B., 2021. Transfer and toxicity of silver nanoparticles in the food chain. Environ. Sci.: Nano. 8, 1519–1535.

de Viedma, M.G., Nelson, M.L., 1977. Notes on insect injection, anesthetization, and bleeding. Great Lakes Entomol. 10 (4), 241–242. https://scholar.valpo.edu/tgle/vol10/iss4/12.

Del Rio, D., Stewart, A.J., Pellegrini, N., 2005. A review of recent studies on malondialdehyde as toxic molecule and biological marker of oxidative stress. Nutr. Metab. Cardiovasc. Dis. 15 (4), 316–328. https://doi.org/10.1016/j.numecd.2005.05.003.

Dexheimer, T.S., 2013. DNA repair pathways and mechanisms. In: Mathews, L.A., Cabarcas, S.M., Hurt, E. (Eds.), DNA Repair for Cancer Stem Cells. Springer, pp. 19–32 https://doi.org/10.1007/978-94-007-4590-2.

Dhawan, A., Bajpayee, M., Parmar, D., 2009. Comet assay: a reliable tool for the assessment of DNA damage in different models. Cell Biol. Toxicol. 25, 5–32. https://doi.org/10.1007/s10565-008-9072-z.

Dziewięcka, M., Karpeta-Kaczmarek, J., Augustyniak, M., Rost-Roszkowska, M., 2017. Short-term in vivo exposure to graphene oxide can cause damage to the gut and testis. J. Hazard. Mater. 328, 80–89. https://doi.org/10.1016/j.jhazmat.2017.01.012.

Dziewięcka, M., Witas, P., Karpeta-Kaczmarek, J., Kwaśniewska, J., Flasz, B., Balin, K., Augustyniak, M., 2018. Reduced fecundity and cellular changes in Acheta domesticus after multigenerational exposure to graphene oxide nanoparticles in food. Sci. Total Environ. 635, 947–955. https://doi.org/10.1016/j.scitotenv.2018.04.207.

Dziewięcka, M., Flasz, B., Rost-Roszkowska, M., Kędziorski, A., Kochanowicz, A., Augustyniak, M., 2020. Graphene oxide as a new anthropogenic stress factor - multigenerational study at the molecular, cellular, individual and population level of Acheta domesticus. J. Hazard. Mater. 396, 122775. https://doi.org/10.1016/j.jhazmat.2020.122775.

El-Ashram, S., Kheirallah, D.A.M., El-Samad, L.M., Toto, N.A., 2020. Relative expression of microRNAs, apoptosis, and ultrastructure anomalies induced by gold nanoparticles in trachyderma hispida (Coleoptera: Tenebrionidae). PLoS One 6;15, e0241837. https://doi.org/10.1371/journal.pone.0241837.

El-Gendy, A.H., Augustyniak, M., Toto, N.A., Al Farraj, S., El-Samad, L.M., 2020. Oxidative stress parameters, DNA damage and expression of HSP70 and MT in midgut of trachyderma hispida (Forskål, 1775) (Coleoptera: Tenebrionidae) from a textile industry area. Environ. Pollut. 267, 115661. https://doi.org/10.1016/j.envpol.2020.115661.

Fang, Y., Dai, M., Ye, W., Li, F., Sun, H., Wei, J., Bing, L., 2021. Damaging effects of TiO2 nanoparticles on the ovarian cells of Bombyx mori. Biol. Trace Elem. Res. https://doi.org/10.1007/s12011-021-02760-9.

Fischer, E.R., Hansen, B.T., Nair, V., Hoyt, F.H., Dorward, D.W., 2012. Scanning electron microscopy. Current Protocols in Microbiology, Chapter 2, Unit2B.2–2B.2 https://doi.org/10.1002/9780471729259.mc02b02s25.

Flasz, B., Dziewięcka, M., Kędziorski, A., Tarnawska, M., Augustyniak, M., 2020. Vitellogenin expression, DNA damage, health status of cells and catalase activity in Acheta domesticus selected according to their longevity after graphene oxide treatment. Sci. Total Environ. 737, 140274. https://doi.org/10.1016/j.scitotenv.2020.140274.

Flasz, B., Dziewięcka, M., Kędziorski, A., Tarnawska, M., Augustyniak, M., 2021. Multigenerational graphene oxide intoxication results in reproduction disorders at the molecular level of vitellogenin protein expression in Acheta domesticus. Chemosphere 280, 130772. https://doi.org/10.1016/j.chemosphere.2021.130772.

Fraczek, M., Hryhorowicz, M., Gaczarzewicz, D., Szumala-Kakol, A., Kolanowski, T.J., Beutin, L., Kurpisz, M., 2015. Can apoptosis and necrosis coexist in ejaculated human spermatozoa during in vitro semen bacterial infection? J. Assist. Reprod. Genet. 32 (5), 771–779. https://doi.org/10.1007/s10815-015-0462-x.

Gajski, G., Žegura, B., Ladeira, C., Novak, M., Sramkova, M., Pourrut, B., Del, C., Milić, M., Bjerve, K., Costa, S., Dusinska, M., Brunborg, G., Collins, A., 2019a. The comet assay in animal models: from bugs to whales - (part 2 vertebrates). Mutat. Res. Mutat. Res. 781, 130–164. https://doi.org/10.1016/j.mrrev.2019.04.002.

Gajski, G., Žegura, B., Ladeira, C., Pourrut, B., Del, C., Novak, M., Sramkova, M., Milić, M., Bjerve, K., Costa, S., Dusinska, M., Brunborg, G., Collins, A., 2019b. The comet assay in animal models: from bugs to whales - (part 1 invertebrates). Mutat. Res. Mutat. Res. 779, 82–113. https://doi.org/10.1016/j.mrrev.2019.02.003.

Garcia, T.X., Costa, G.M., França, L.R., Hofmann, M.C., 2014. Sub-acute intravenous administration of silver nanoparticles in male mice alters leydig cell function and testosterone levels. Reprod. Toxicol. 45, 59–70. https://doi.org/10.1016/j.reprotox.2014.01.006.

Gil, P., Fariñas, F., Casado, A., López-Fernández, E., 2002. Malondialdehyde: a possible marker of ageing. Gerontology 48 (4), 209–214. https://doi.org/10.1159/000058352.

Gromadzka-Ostrowska, J., Dziendzikowska, K., Lankoff, A., Dobrzyńska, M., Instanes, C., Brunborg, G., Gajowik, A., Radzikowska, J., Wojewódzka, M., Kruszewski, M., 2012. Silver nanoparticles effects on epididymal sperm in rats. Toxicol. Lett. 214 (3), 251–258. https://doi.org/10.1016/j.toxlet.2012.08.028.

Guo, Z., Cui, K., Zeng, G., Wang, J., Guo, X., 2018. Silver nanomaterials in the natural environment: an overview of their biosynthesis and kinetic behavior. Sci. Total Environ. 643, 1325–1336. https://doi.org/10.1016/j.scitotenv.2018.06.302.

Hoseini-Alfatemi, S., Fallah, F., Armin, S., Hafizi, M., Karimi, A., Kalanaky, S., 2020. Evaluation of blood and liver cytotoxicity and apoptosis-necrosis induced by nanochelating based silver nanoparticles in mouse model. Iran J. Pharm. Res. 19 (2), 207–218. https://doi.org/10.22037/ijpr.2020.1101026.

Husain, W.M., Araak, J.K., Ibrahim, O.M.S., 2019. Effect of zinc oxide nanoparticles on sperm cell comet assay, testis malondialdehyde and glutathione peroxidase levels in adult rats. Online J. Vet. 23, 206–213.

Inagaki, Y., Matsumoto, Y., Kataoka, K., Matsuhashi, N., Sekimizu, K., 2012. Evaluation of drug-induced tissue injury by measuring alanine aminotransferase (ALT) activity in silkworm hemolymph. BMC Pharmacol. Toxicol. 13, 13. https://doi.org/10.1186/2050-6511-13-13.

Kanduc, D., Mittelman, A., Serpico, R., Sinigaglia, E., Sinha, A.A., Natale, C., Santacroce, R., Di Corcia, M.G., Lucchese, A., Dini, L., Pani, P., Santacroce, S., Simone, S., Bucci, R., Farber, E., 2002. Cell death: apoptosis versus necrosis (review). Int. J. Oncol. 21 (1), 165–170.

Karpeta-Kaczmarek, J., Dziewięcka, M., Augustyniak, M., Rost-Roszkowska, M., Pawlyta, M., 2016. Oxidative stress and genotoxic effects of diamond nanoparticles. Environ. Res. 148, 264–272. https://doi.org/10.1016/j.envres.2016.03.033.

Karpeta-Kaczmarek, J., Kędziorski, A., Augustyniak-Jabłokow, M.A., Dziewięcka, M., Augustyniak, M., 2018. Chronic toxicity of nanodiamonds can disturb development and reproduction of Acheta domestica L. Environ. Res. 166, 602–609. https://doi.org/10.1016/j.envres.2018.05.027.

Kheirallah, D.A.M., El-Samad, L.M., 2019b. Spermatogenic alterations in the ground beetle trachyderma hispida (Coleoptera: Tenebrionidae) induced by ceramic industrial pollution. Afr. Entomol. 27 (2), 418–432. https://doi.org/10.4001/003.027.0418.

Kheirallah, D.A.M., El-Samad, L.M., Mokhamer, E.H.M., Abdul-Aziz, K.K., Toto, N.A.H., 2019a. DNA damage and oogenesis anomalies in pimelia latreillei (Coleoptera: Tenebrionidae) induced by heavy metals soil pollution. Toxicol. Ind. Health 35 (11–12), 688–702. https://doi.org/10.1177/0748233719893200.

Kheirallah, D.A., El-Samad, L.M., Abdel-Moneim, A.M., 2021. DNA damage and ovarian ultrastructural lesions induced by nickel oxide nano-particles in blaps polycresta (Coleoptera: Tenebrionidae). Sci. Total Environ. 753, 141743. https://doi.org/10.1016/j.scitotenv.2020.141743.

Khodaparast, Z., van Gestel, C.A.M., Papadiamantis, A.G., Gonçalves, S.F., Lynch, I., Loureiro, S., 2021. Toxicokinetics of silver nanoparticles in the mealworm Tenebrio molitor exposed via soil or food. Sci. Total Environ. 777, 146071. https://doi.org/10.1016/j.scitotenv.2021.146071.

Koopman, G., Reutelingsperger, C.P., Kuijten, G.A., Keehnen, R.M., Pals, S.T., van Oers, M.H., 1994. Annexin V for flow cytometric detection of phosphatidylserine expression on B cells undergoing apoptosis. Blood 184 (5), 1415–1420.

Krysko, D.V., Vanden Berghe, T., D'Herde, K., Vandenabeele, P., 2008. Apoptosis and necrosis: detection, discrimination and phagocytosis. Methods 44 (3), 205–221. https://doi.org/10.1016/j.ymeth.2007.12.001.

Lafuente, D., Garcia, T., Blanco, J., Sánchez, D.J., Sirvent, J.J., Domingo, J.L., Gómez, M., 2016. Effects of oral exposure to silver nanoparticles on the sperm of rats. Reprod. Toxicol. 2016 (60), 133–139. https://doi.org/10.1016/j.reprotox.2016.02.007.

Leclerc, L., Klein, J.P., Forest, V., Boudard, D., Martini, M., Pourchez, J., Blanchin, M.G., Cottier, M., 2015. Testicular biodistribution of silica-gold nanoparticles after intramuscular injection in mice. Biomed. Microdevices 17 (4), 66. https://doi.org/10.1007/s10544-015-9968-3.

Leonard, C., Söderhäll, K., Ratcliffe, N.A., 1985. Studies on prophenoloxidase and protease activity of Blaberus craniifer haemocytes. Insect Biochem. 15 (6), 803–810.. https://doi.org/10.1016/0020-1790(85)90109-X.

Łoś, A., Strachecka, A., 2018. Fast and cost-effective biochemical spectrophotometric analysis of solution of insect "Blood" and body surface elution. Sensors (Basel) 18 (5), 1494. https://doi.org/10.3390/s18051494.

Lowry, O.H., Rosebrough, N.J., Farr, A.L., Randall, R.J., 1951. Protein measurement with the folin phenol reagent. J. Biol. Chem. 193, 265–275.

McGillicuddy, E.M., Murray, I., Kavanagh, S., Morrison, L., Fogarty, A., Cormican, M., Dockery, P., Prendergast, M., Rowan, N., Morris, D., 2017. Silver nanoparticles in the environment: sources, detection and ecotoxicology. Sci. Total Environ. 575, 231–246. https://doi.org/10.1016/j.scitotenv.2016.10.041.

McShan, D., Ray, P.C., Yu, H., 2014. Molecular toxicity mechanism of nanosilver. J. Food Drug Anal. 22 (1), 116–127. https://doi.org/10.1016/j.jfda.2014.01.010.

Misra, H.P., Fridovich, I., 1972. The role of superoxide anion in the autoxidation of epinephrine and a simple assay for superoxide dismutase. J. Biol. Chem. 247, 3170–3175.

Ni, M., Li, F., Wang, B., Xu, K., Zhang, H., Hu, J., Tian, J., Shen, W., Li, B., 2015. Effect of TiO2 nanoparticles on the reproduction of silkworm. Biol. Trace Elem. Res. 164 (1), 106–113. https://doi.org/10.1007/s12011-014-0195-1.

O'Donnell, B., Huo, L., Polli, J.R., Qiu, L., Collier, D.N., Zhang, B., Pan, X., 2017. From the cover: ZnO nanoparticles enhanced germ cell apoptosis in Caenorhabditis elegans, in comparison with ZnCl2. Toxicol. Sci. 156 (2), 336–343. https://doi.org/10.1093/toxsci/kfw258.

Ohkawa, K., Ohishi, W., Yagi, K.A., 1979. Assay for lipid peroxides in animal tissues by thiobarbituric acid reaction. Anal. Biochem. 95, 351–358. https://doi.org/10.1016/0003-2697(79)90738-3.

Osman, W., Shonouda, M., 2017. X-ray metal assessment and ovarian ultrastructure alterations of the beetle, blaps polycresta (Coleoptera, Tenebrionidae), inhabiting polluted soil. Environ. Sci. Pollut. Res. 24, 14867–14876. https://doi.org/10.1007/s11356-017-9095-1.

Osman, W., El-Samad, L.M., Mokhamer, el-H., El-Touhamy, A., Shonouda, M., 2015. Ecological, morphological, and histological studies on Blaps polycresta (Coleoptera: Tenebrionidae) as biomonitors of cadmium soil pollution. Environ. Sci. Pollut. Res. Int. 22 (18), 14104–14115. https://doi.org/10.1007/s11356-015-4606-4.

Paglia, E.D., Valentine, W.N., 1967. Studies on quantitative and qualitative characterization of erythrocyte peroxidases. J. Lab. Clin. Med. 70 (1), 158–164.

Plata-Rueda, A., Rolim, G.D.S., Wilcken, C.F., Zanuncio, J.C., Serrão, J.E., Martínez, L.C., 2020. Acute toxicity and sublethal effects of lemongrass essential oil and their components against the Granary Weevil, Sitophilus granarius. Insects 11 (6), 379. https://doi.org/10.3390/insects11060379.

Pulit-Prociak, J., Banach, M., 2016. Silver nanoparticles – a material of the future? Open Chem. 14, 76–91. https://doi.org/10.1515/chem-2016-0005.

Rai, M., Yadav, A., Gade, A., 2009. Silver nanoparticles as a new generation of antimicrobials. Biotechnol. Adv. 27, 76–83. https://doi.org/10.1016/j.biotechadv.2008.09.002.

Raj, A., Shah, P., Agrawal, N., 2017. Dose-dependent effect of silver nanoparticles (AgNPs) on fertility and survival of drosophila: an in-vivo study. PLoS One. 12 (5), e0178051. https://doi.org/10.1371/journal.pone.0178051.

Reynolds, E.S., 1963. The use of lead citrate at high pH as an electronopaque stain in electron microscopy. J. Cell Biol. 17, 208–212. https://doi.org/10.1083/jcb.17.1.208.

Seyed Alian, R., Dziewięcka, M., Kędziorski, A., Majchrzycki, Ł., Augustyniak, M., 2021. Do nanoparticles cause hormesis? Early physiological compensatory response in house

crickets to a dietary admixture of GO, ag, and GOAg composite. Sci. Total Environ. 788, 147801. https://doi.org/10.1016/j.scitotenv.2021.147801.

Shevlin, D., O'Brien, N., Cummins, E., 2018. Silver engineered nanoparticles in freshwater systems - likely fate and behaviour through natural attenuation processes. Sci. Total Environ. 621, 1033–1046. https://doi.org/10.1016/j.scitotenv.2017.10.123.

Singh, N.P., McCoy, M.T., Tice, R.R., Schneider, E.L., 1988. A simple technique for quantitation of low levels of DNA damage in individual cells. Exp. Cell Res. 175, 184–191. https://doi.org/10.1016/0014-4827(88)90265-0.

Soldati, L., Condamine, F.L., Clamens, A., Kergoat, G.J., 2017. Documenting tenebrionid diversity: progress on blaps fabricius (Coleoptera, tenebrionidae, tenebrioninae, Blaptini) systematics, with the description of five new species. Eur. J. Taxo. 282, 1–29.. https://doi:10.5852/ejt.2017.282.

Tortella, G.R., Rubilar, O., Durán, N., Diez, M.C., Martínez, M., Parada, J., Seabra, A.B., 2020. Silver nanoparticles: toxicity in model organisms as an overview of its hazard for human health and the environment. J. Hazard. Mater. 390, 121974. https://doi.org/10.1016/j.jhazmat.2019.121974.

Wang, R., Song, B., Wu, J., Zhang, Y., Chen, A., Shao, L., 2018. Potential adverse effects of nanoparticles on the reproductive system. Int. J. Nanomedicine 13, 8487–8506. https://doi.org/10.2147/IJN.S170723.

Wei, L., Lu, J., Xu, H., Patel, A., Chen, Z.S., Chen, G., 2015. Silver nanoparticles: synthesis, properties, and therapeutic applications. Drug Discov. Today 20 (5), 595–601. https://doi.org/10.1016/j.drudis.2014.11.014.

Yousef, H.A., Abdelfattah, E.A., Augustyniak, M., 2019. Antioxidant enzyme activity in responses to environmentally induced oxidative stress in the 5th instar nymphs of aiolopus thalassinus (Orthoptera: Acrididae). Environ. Sci. Pollut. Res. Int. 26 (4), 3823–3833. https://doi.org/10.1007/s11356-018-3756-6.

Yu, S.J., 1982. Host plant induction of glutathione S-transferase in the fall armyworm. Pestic Biochem. Phys. 18, 101–106. https://doi.org/10.1016/0048-3575(82)90092-X.

Yu, S.J., Hsu, E.L., 1993. Induction of detoxification enzymes in phytophagous insects: roles of insecticide synergists, larval age, and species. Arch. Insect Biochem. Physiol. 24, 21–32. https://doi.org/10.1002/arch.940240103.